

This discussion paper is/has been under review for the journal Hydrology and Earth System Sciences (HESS). Please refer to the corresponding final paper in HESS if available.

Spectral representation of the annual cycle in the climate change signal

T. Bosshard¹, S. Kotlarski¹, T. Ewen^{1,*}, and C. Schär¹

¹Institute for Atmospheric and Climate Science, ETH Zurich, Zurich, Switzerland
*now at: Department of Geography, University of Zurich, Zurich, Switzerland

Received: 26 December 2010 – Accepted: 3 January 2011 – Published: 26 January 2011

Correspondence to: T. Bosshard (thomas.bosshard@env.ethz.ch)

Published by Copernicus Publications on behalf of the European Geosciences Union.

HESSD

8, 1161–1192, 2011

**Spectral
representation of the
annual cycle in the
climate change signal**

T. Bosshard et al.

Title Page

Abstract

Introduction

Conclusions

References

Tables

Figures

⏪

⏩

◀

▶

Back

Close

Full Screen / Esc

Printer-friendly Version

Interactive Discussion

Abstract

The annual cycle of temperature and precipitation changes as projected by climate models is of fundamental interest in climate impact studies. Its estimation, however, is impaired by natural variability. Using a simple form of the delta change method, we show that on regional scales relevant for hydrological impact models, the projected changes in the annual cycle are prone to sampling artefacts. For precipitation at station locations, these artefacts may have amplitudes that are comparable to the climate change signal itself. Therefore, the annual cycle of the climate change signal should be filtered when generating climate change scenarios. We test a spectral smoothing method to remove the artificial fluctuations. Comparison against moving monthly averages shows that sampling artefacts in the climate change signal can successfully be removed by spectral smoothing. The method is tested at Swiss climate stations and applied to regional climate model output of the ENSEMBLES project. The spectral method performs well, except in cases with a strong annual cycle and large relative precipitation changes.

1 Introduction

Impacts of climate change on the hydrological cycle are both of high scientific interest as well as of high relevance for society as a whole. The former is due to the intimate coupling of the hydrological cycle and the climate system (Allen and Ingram, 2002; Wentz et al., 2007; Wild et al., 2008) while the latter is based on the manifold interactions between the anthroposphere and the hydrosphere (Kundzewicz et al., 2007). Hydrological impact studies focussing on runoff often use statistically post-processed global climate model (GCM) or regional climate model (RCM) data to drive a hydrological model (Hay et al., 2000; Leung et al., 2004; Wood et al., 2004; Kay et al., 2006; Buytaert et al., 2010). For this purpose, various statistical post-processing methods have been developed (see e.g. Fowler et al., 2007, for a comprehensive review). All

HESSD

8, 1161–1192, 2011

Spectral representation of the annual cycle in the climate change signal

T. Bosshard et al.

Title Page

Abstract

Introduction

Conclusions

References

Tables

Figures

⏪

⏩

◀

▶

Back

Close

Full Screen / Esc

Printer-friendly Version

Interactive Discussion

these methods are based on statistical relationships that bridge the spatial and temporal gaps between observations and modelled data, and attempt to correct for climate model biases. Most of the available methods focus on the hydrometeorological variables temperature and precipitation (abbreviated as T and P , respectively in the remainder of this article) and usually include some representation of the annual cycle.

Natural variability, both on interannual as well as intraannual time scales, impairs parameter estimates of the statistical post-processing methods. The range of the natural variability can be assessed using e.g. resampling techniques. Prudhomme and Davies (2009) and Wood et al. (2004), for example, resampled observed time series to estimate the range of natural variability of the climate change signal. Cross-validation has also been used to test the robustness of the parameter estimates to interannual variability (Terink et al., 2010; Schmidli et al., 2007; Widmann et al., 2003). However, only a few studies focussing on hydrological impacts have looked in detail at the intraannual variability of the parameters. Smoothing by averaging over seasons (see e.g. Schmidli et al., 2007) or months (see e.g. Middelkoop et al., 2001; Kleinn et al., 2005), is a common practise. An appropriate representation of the seasonal cycle, however, is not straightforward. On the one hand, the optimal choice of the averaging period is dependent on the magnitude of the natural variability, the spatial averaging and the length of the data records. The stronger the natural variability, the smaller the spatial averaging area and the shorter the data record is, the wider the averaging window has to be chosen in order to reduce the effects of natural variability on the parameter estimates. On the other hand, hydrological impact modellers are interested in an accurate representation of the annual cycle and therefore prefer as narrow averaging windows as feasible. The optimal solution is thus not trivial to find and is case dependent. Despite its importance, the discussion of how to optimally represent the annual cycle in climate change scenarios is often neglected in recent impact modelling. In many cases, the averaging window width is mentioned without specific justification (e.g. Cameron et al., 2000; Jasper et al., 2004; Graham et al., 2007).

Spectral representation of the annual cycle in the climate change signal

T. Bosshard et al.

[Title Page](#)

[Abstract](#)

[Introduction](#)

[Conclusions](#)

[References](#)

[Tables](#)

[Figures](#)



[Back](#)

[Close](#)

[Full Screen / Esc](#)

[Printer-friendly Version](#)

[Interactive Discussion](#)



**Spectral
representation of the
annual cycle in the
climate change signal**T. Bosshard et al.

[Title Page](#)[Abstract](#)[Introduction](#)[Conclusions](#)[References](#)[Tables](#)[Figures](#)[Back](#)[Close](#)[Full Screen / Esc](#)[Printer-friendly Version](#)[Interactive Discussion](#)

This paper elaborates on the representation of the annual cycle in the climate change signal within the delta change post-processing methodology. We chose the delta change method because of its simplicity, but the results appear relevant for more sophisticated methods as well. The delta change method has been used for hydrological impact studies ever since GCM data became available, and it is still used nowadays (Gleick, 1986; Hay et al., 2000; Prudhomme et al., 2002; Lenderink et al., 2007). More sophisticated combinations of the delta change approach and weather generators have also been developed (Kilsby et al., 2007). It is noteworthy that Gleick (1986) already stressed the importance of representing the climate change throughout the annual cycle since seasonal changes tend to cancel each other out in the annual average.

Here, we test the influence of sampling variability on the annual cycle of the climate change signal by using moving averages (MA) of different window widths. As an alternative to the MA, we present a spectral approach to estimate the climate change signal. The spectral estimation produces smoother annual cycles of the climate change signals than MAs. Our analysis is carried out at observational station sites in Switzerland.

The paper is structured as follows: in Sect. 2, we present the data used for the study. Section 3 introduces the delta change method and the estimation methods for the annual cycle. In Sect. 4, we study the effects of sampling variability on the estimation of the annual cycle using a stochastic rainfall generator. Section 5 presents the estimation of the annual cycle of the climate change signal using a spectral smoothing method and a comparison to estimates using MAs of 31 days window width. Results at Swiss station sites are shown at the end of this section. Section 6 summarises the findings and discusses their relevance for climate impact studies.

2 Data

We used daily near-surface T and P data from 10 GCM-RCM model chains provided by the ENSEMBLES project (van der Linden and Mitchell, 2009) to estimate the annual cycle of the climate change signal (see Table 1). All model chains use the A1B emission

scenario, cover the period 1951–2099 and have a horizontal resolution of about 25 km. We had to exclude the HadCM3Q16 driven model chains due to pronounced summer dryings that caused severe overshooting in the spectral smoothing (see Sect. 5.2 for an explanation).

The geographical focus of our study is Switzerland. Throughout this paper, the estimation of the climate change signal is based on RCM data interpolated to station locations of MeteoSwiss (see Fig. 1). All the stations provide T and P data with at least daily resolution in the period 1980–2009. We used the four nearest gridpoints and the inverse distance weighting interpolation algorithm to spatially interpolate the GCM-RCM data to station locations. It should also be noted that any height correction is redundant since constant correction terms cancel each other in the delta change approach. Also, for simplicity, we neglect leap days in the data, unless stated otherwise.

For the stochastic rainfall generator experiments, two subsets of precipitation stations are used to estimate the rainfall generator parameters. These subsets are indicated by blue and red dots in Fig. 1 (see also Sect. 4). In addition, we used long-term data series from 26 stations with records going back to 1900 from the climate monitoring network of MeteoSwiss to constrain the harmonic smoothing model. Stars mark these stations in Fig. 1.

3 Methodology

3.1 The delta change method

The delta change method scales station records according to a climate change signal. The climate change signal is usually derived from climate model data as the change between a scenario period (SCE) and a control period (CTL). As a result of the scaling, the spatio-temporal patterns as well as the correlations between the variables closely follow the observed records. Thus, the delta change method is considered a robust method to generate climate impact scenarios (Graham et al., 2007).

Spectral representation of the annual cycle in the climate change signal

T. Bosshard et al.

Title Page

Abstract

Introduction

Conclusions

References

Tables

Figures

⏪

⏩

◀

▶

Back

Close

Full Screen / Esc

Printer-friendly Version

Interactive Discussion



In this study, we applied the delta change method at station sites for the SCE periods 2021–2050 and 2070–2099, both relative to the CTL period 1980–2009. At each station i , for each RCM j and for each day d in the year, we estimate the mean annual cycle of the variable of interest and denote it with $\overline{X_{i,j}^{\text{CTL}}}(d)$ for the control and $\overline{X_{i,j}^{\text{SCE}}}(d)$ for the scenario period where X stands for either T or P . The delta change method then derives an additive ($\Delta X_{i,j}^{\text{add}}(d)$) and a multiplicative ($\Delta X_{i,j}^{\text{mult}}(d)$) climate change signal for T and P , respectively, according to

$$\Delta T_{i,j}^{\text{add}}(d) = \overline{T_{i,j}^{\text{SCE}}}(d) - \overline{T_{i,j}^{\text{CTL}}}(d) \quad (1)$$

$$\Delta P_{i,j}^{\text{mult}}(d) = \frac{\overline{P_{i,j}^{\text{SCE}}}(d)}{\overline{P_{i,j}^{\text{CTL}}}(d)}. \quad (2)$$

Let $X_{i,\text{obs}}^{\text{CTL}}(y, d)$ denote the continuous observational time series at station sites in the CTL period 1980–2009. Here, y represents the years in the CTL period. In the delta change method, all observational time steps in the CTL period belonging to the same day d in the year are scaled with the corresponding climate change value. Again, one commonly uses an additive or multiplicative scaling for T and P , respectively:

$$T_{i,j}^{\text{SCE,add}}(y, d) = T_{i,\text{obs}}^{\text{CTL}}(y, d) + \Delta T_{i,j}^{\text{add}}(d) \quad (3)$$

$$P_{i,j}^{\text{SCE,mult}}(y, d) = P_{i,\text{obs}}^{\text{CTL}}(y, d) \cdot \Delta P_{i,j}^{\text{mult}}(d) \quad (4)$$

Equations (1)–(4) reveal that a key issue in the delta change approach is the estimation of the climatological annual cycle in a predefined period. In fact, the delta change approach states nothing but how the climatological annual cycle changes in the transition of the atmospheric state between a CTL and SCE period according to climate model simulations. If one fails to estimate a robust annual cycle in either the CTL or the SCE period, one will fail to project an accurate change of the annual cycle.

Spectral representation of the annual cycle in the climate change signal

T. Bosshard et al.

Title Page

Abstract

Introduction

Conclusions

References

Tables

Figures

⏪

⏩

◀

▶

Back

Close

Full Screen / Esc

Printer-friendly Version

Interactive Discussion



3.2 Estimation of the climatological annual cycle

It is not possible to derive the true climatological annual cycle of any variable but only an estimate thereof, due to the natural variability and the limited duration of observed or simulated data records. The uncertainty of the estimate might be represented by a stochastic component. Ideally, the estimated climatological annual cycle should be robust and not depend on the stochastic components in the time series while preserving the amplitude of the annual cycle. Often, the optimisation of these criteria is a trade-off, and it is not trivial to choose an optimal method to estimate the climatological annual cycle.

In this study, we used MAs and a spectral approach as an alternative to the MA for the estimation of the climatological annual cycle of T and P . In the MA approach, the terms $\overline{X(d)}_{\text{mod}}^{\text{CTL}}$ and $\overline{X(d)}_{\text{mod}}^{\text{SCE}}$ in Eqs. (1) and (2) become

$$\overline{X_{i,j}}(d) = \frac{1}{y_e - y_s + 1} \sum_{y=y_s}^{y_e} \left[\frac{1}{2n+1} \sum_{k=d-n}^{d+n} X_{i,j}(y, k) \right] \quad (5)$$

where y_s and y_e denote the start and end year of the chosen period and n stands for the number of days before and after the day d in each year y . We used MAs with window widths of 15 ($n=7$), 31 ($n=15$), 61 ($n=30$) and 91 ($n=45$) days. The larger the n , the smaller the effect of the natural variability on the estimate of the climatological annual cycle. However, the amplitude of the annual cycle is more strongly damped for larger n .

In the alternative spectral approach, we investigated a spectral reconstruction of the climatological annual cycle by a superposition of harmonics with the base period $P = 365$ d.

$$\overline{X_{i,j}}(d) = a_{i,j}^0 + \sum_{k=1}^H [a_{i,j}^k \cos(\omega^k d) + b_{i,j}^k \sin(\omega^k d)] \quad (6)$$

$$\omega^k = \frac{2k\pi}{P} \quad (7)$$

Spectral representation of the annual cycle in the climate change signal

T. Bosshard et al.

Title Page

Abstract

Introduction

Conclusions

References

Tables

Figures

⏪

⏩

◀

▶

Back

Close

Full Screen / Esc

Printer-friendly Version

Interactive Discussion



The superscript k indicates the order of the harmonic components and H is the maximum order retained. The coefficients $a_{i,j}^k$ and $b_{i,j}^k$ are estimated using the discrete Fourier transform (see e.g. von Storch and Zwiers, 1999) from the daily time series of the RCM j at station site i in the CTL and SCE period.

For RCMs using the Gregorian calendar, the base period P is set to 365.25 to account for leap years (Narapusetty et al., 2009). The HadCM3Q0 and HadCM3Q3 driven RCMs have a 360 days calendar. For these RCMs, we set P to 360 days. Having estimated the harmonically smoothed climatological cycle at each station site and for each RCM, we scale the different lengths of the annual cycle to fit 365 days by choosing $P = 365$ in the reconstruction of $\overline{X_{i,j}}(d)$ as in Eq. (6).

In the spectral framework of harmonics, the choice of the maximum order H is the only free parameter. The larger H is, the more the details of the annual cycle can be resolved, but the more vulnerable the spectral model becomes to influences of natural variability and overfitting.

4 Analysis of synthetically generated precipitation time series

Let's assume we could sample two 30 year long precipitation time series from a stationary climate and derive the annual cycle of the precipitation change between the two time series. Stationary here means that the mean climate state is the same in both samples, but the two realisations are modulated by natural variability. Since we know that the climate is stationary by assumption, the asymptotic solution of the precipitation change (expressed as a ration) should equal one representing no precipitation change. Any deviation from one, e.g., the occurrence of an annual cycle in the precipitation change signal, is solely caused by sampling variability, and does not contain any climate signal.

Here, we investigate the degree of the sampling artefacts in the annual cycle of precipitation in an idealised stochastic setup using a rainfall generator with stationary parameters. The setup consists of four experiments which are representative for

Spectral representation of the annual cycle in the climate change signal

T. Bosshard et al.

Title Page

Abstract

Introduction

Conclusions

References

Tables

Figures

⏪

⏩

◀

▶

Back

Close

Full Screen / Esc

Printer-friendly Version

Interactive Discussion



precipitation series of individual station sites (STATION) and regions (REGION) both for the northern (CHN) and southern (CHS) parts of Switzerland, in order to study two distinct climates at station and regional scale. Following Wilks and Wilby (1999), we employed a first order Markov chain rainfall generator with the precipitation intensity being modelled by a two-parameter gamma distribution. Let p_{dw} and p_{ww} be the transition probabilities from a dry to wet and a wet to wet day, respectively. Given realisations of the uniform random number on the unit interval r_1 , the precipitation occurrence $Y(t)$ is modelled as

$$Y(t) = \begin{cases} 1 & \text{if } Y(t-1) = 0 \text{ and } r_1 \leq p_{dw} \\ 1 & \text{if } Y(t-1) = 1 \text{ and } r_1 \leq p_{ww} \\ 0 & \text{otherwise} \end{cases} \quad (8)$$

where 1 stands for a wet and 0 for a dry day. On wet days, the precipitation intensity $I(t)$ is sampled from a gamma probability density function according to

$$f(I(t)) = \frac{(I(t)/\beta)^{(\alpha-1)} e^{(-I(t)/\beta)}}{\beta \Gamma(\alpha)}, \quad I(t), \alpha, \beta > 0 \quad (9)$$

where α and β are parameters of the gamma distribution and Γ is the gamma function. In this case, the synthetic precipitation time series P_{synth} is derived as

$$P_{\text{synth}}(t) = Y(t) \cdot I(t) \quad (10)$$

For the single-station experiments CHN_{STATION} and CHS_{STATION} , we derived the parameters p_{dw} , p_{ww} , α and β from the observed daily precipitation records in the period 1980–2009 at the stations Bern (BER) and Lugano (LUG), respectively. The parameters were estimated for each season separately. At the transition from one season to the other, the parameter set is changed but the wet/dry state from the last day of the previous season is taken for the continuation of the Markov chain.

For the experiments representing regional precipitation, we first selected all stations in a radius r around BER ($r = 60$ km) and LUG ($r = 40$ km) that have less than 10%

Spectral representation of the annual cycle in the climate change signal

T. Bosshard et al.

Title Page

Abstract

Introduction

Conclusions

References

Tables

Figures

⏪

⏩

◀

▶

Back

Close

Full Screen / Esc

Printer-friendly Version

Interactive Discussion



missing values in the period 1980–2009 and calculated the mean daily precipitation time series therefrom. Remaining missing data were ignored in the averaging. The selected stations are indicated by red and blue dots in Fig. 1. We are aware that this averaging does not follow any spatial interpolation standards. The procedure suffices, though, to analyse the effect of spatial averaging on the fluctuations of the climate change signal. Table 2 lists the seasonal parameter settings for each of the four experiments.

For each experiment, we generated 100 realisations of a daily precipitation time series with a length of 30 years. Subsequently, we randomly chose 500 pairs out of the 100 realisations and calculated the multiplicative precipitation change signal by MAs with window widths of 15, 31, 61 and 91 days. The results are shown in Fig. 2. Since both time series of each pair have been generated with the same rainfall generator settings, the asymptotic solution is one, indicating no change. The dots in Fig. 2 display one randomly chosen realisation of the synthetically generated climate change signal ΔP_{synth} using different MA window widths. The 15d MA estimate shows large fluctuations in every experiment. The wider the MA window becomes, the smaller the fluctuations get. The 31d MA, corresponding to a monthly resolution, is a standard averaging window length in many impact studies. In the 31d MA estimates, the amplitudes of the ΔP_{synth} fluctuations are typically in the order of 0.2, but the amplitudes of spikes can be as large as 0.3 as in the case of CHS_{STATION}. The grey bands depict the 10th–90th% quantile range of the 500 realisations.

Comparison of upper and lower panels in Fig. 2 shows that the spatial averaging does not reduce the band width of the 10th–90th% quantile range substantially. In the CHN experiments, spatial averaging reduces the width of the 31d MA band averaged over the year from 0.87–1.15 to 0.89–1.12 whereas in the CHS cases, the width is reduced from 0.82–1.22 to 0.84–1.19.

The results indicate that on station scale as well as on regional scales relevant for hydrological impact studies, the fluctuations of ΔP arising from sampling variability alone have to be considered in interpretations of climate change signals. The exact range of

Spectral representation of the annual cycle in the climate change signal

T. Bosshard et al.

Title Page

Abstract

Introduction

Conclusions

References

Tables

Figures



Back

Close

Full Screen / Esc

Printer-friendly Version

Interactive Discussion



the sampling variability is dependent on the averaging window width, the spatial scale, the region of interest and the length of the climate records. For 31d MAs, our analysis shows for representative climate regions of Switzerland, that ΔP values in the range of 0.8 to 1.2 could be solely caused by sampling variability and do not necessarily contain a climate change signal. Furthermore, the spikes within the annual cycles of ΔP call for estimation methods that produce smoother climatological annual cycles than MAs.

5 Analysis of the climate change signal from regional climate model at Swiss station sites

The stochastic analysis in Sect. 4 revealed that for variables having similar characteristics as P , like e.g. a clustering of events and a heavily skewed intensity distribution, estimates of the climate change signal using MAs are prone to substantial artificial fluctuations caused by natural variability. In particular, such fluctuations lead to an impaired representation of the minima and maxima in the annual cycle of the climate change signal. Harmonic smoothing is able to filter these fluctuations. However, the maximal order of the harmonic smoothing model (see Eq. 6) needs to be chosen. In this section we first define the optimal order of the harmonic smoothing model for T and P . We then present a qualitative comparison between the harmonic and the 31d MA estimates of the climate change signal at station sites, since monthly averaging periods are often employed in climate impact studies. Finally, we show the climate change signals of T and P estimated by harmonic smoothing for 10 GCM-RCM chains at station sites in Switzerland.

5.1 Estimation of the optimal harmonic model

We use long-term observational station records of the Swiss climate monitoring network to constrain the maximum order of the harmonic smoothing model which is then

Spectral representation of the annual cycle in the climate change signal

T. Bosshard et al.

Title Page

Abstract

Introduction

Conclusions

References

Tables

Figures

⏪

⏩

◀

▶

Back

Close

Full Screen / Esc

Printer-friendly Version

Interactive Discussion



applied to GCM-RCM series. This approach implicitly assumes that signal components from GCM-RCM time series having a higher frequency than the optimal harmonic order are considered as being noise. We use a cross-validation technique to specify the harmonic order for the annual cycle that optimally represents the time series. The methodology is described in detail in Narapusetty et al. (2009). Here, we give only a brief introduction and present our specific setup.

We extracted 30 year time slices from 25 temperature and 26 precipitation station records with daily resolution, and split them into ten blocks of three year lengths. Five different 30 year time windows are analysed in order to test the robustness of the results with respect to decadal variability. At each station and for each order of the harmonic smoothing model, we carry out a 10-fold cross-validation by calibrating the harmonic model on 9 of the 10 blocks and validating it on the remaining block. The goal of the cross-validation is to estimate the harmonic model that has the lowest estimated prediction error (EPE). The EPE is a measure of the model error in an independent data set that was not used for calibration. It therefore penalises models that are overfitting the data. We use the mean squared error (MSE) as a measure for the EPE and call it the cross-validated MSE (MSE_{CV}). The MSE_{CV} is optimal for normally distributed and independent residuals. P time series however show strongly non-normal residual distributions. This might cause the estimation of the optimal model to be biased. We therefore first carried out a Box-Cox transformation (Wilks, 2006, p. 43) on the P data. The Box-Cox transformation is a one parametric power-transformation that scales random variables in a way that their distribution becomes symmetric. Since the Box-Cox transformation only works on positive definite variables, we replaced zeros in the P data by 0.0001.

Figures 3 and 4 show the results of the cross-validation. For T , the MSE_{CV} drops to a low level at the harmonic order (HO) of 2 and remains on this low level up to HO 8. Within this plateau, the differences between the models in terms of the MSE_{CV} are small. Depending on the analysis period, the order with the lowest MSE_{CV} varies between HO 2 and HO 8. The MSE_{CV} starts to consistently increase again for higher

Spectral representation of the annual cycle in the climate change signal

T. Bosshard et al.

Title Page

Abstract

Introduction

Conclusions

References

Tables

Figures



Back

Close

Full Screen / Esc

Printer-friendly Version

Interactive Discussion



orders than HO 8. In the case of P , the MSE_{CV} has a minimum at HO 2, but the difference to HO 3 is very small. This result is robust for different analysis periods.

The above analysis yields different optimal harmonic orders for T and P . However, as the two atmospheric variables are linked through dynamical and thermodynamical processes, the optimal order for both variables should preferably be the same. We thus chose HO 3 as the optimal order for T and P . With a higher joint HO, we would accept higher-frequency precipitation fluctuations that could stem from natural variability rather than climate change.

5.2 Comparison between the moving average and the spectral estimation of the climate change signal

Based on the results in Sect. 5.1, we use a third order harmonic model (HO 3) to estimate the annual cycle of P and T in the CTL and SCE periods and compare it to 31d MA estimates. We expect the HO 3 estimates to be characterised by smoother annual cycles and smaller peaks in the annual cycle than 31d MA estimates.

For illustration, Fig. 5 displays annual cycles of P and T at the two station sites BER and LUG as modelled by ETHZ-HadCM3Q0-CLM in the CTL period and the SCE period 2070–2099 as well as the climate change signal (lower panels). These two stations and the selected model chain represent typical results. The annual cycle of the observed values in the CTL period is shown in grey.

In the case of T , the annual cycle is well captured at both stations, although biases of up to 2 K arise for individual months. The fluctuations in the 31d MA estimate of ΔT have a time scale of typically one month. The amplitudes of these fluctuations are in the order of 0.5–1 K. The HO 3 estimate treats these fluctuations as noise and results in a smooth annual cycle of ΔT .

The depicted precipitation shows a large bias in winter on the northern side of the Alps (BER), whereas in southern Switzerland (LUG), the RCM is able to reproduce the two precipitation peaks in the annual cycle but has a biased amplitude. Such biases are not uncommon in regions of complex topography. For a detailed evaluation of

Spectral representation of the annual cycle in the climate change signal

T. Bosshard et al.

Title Page

Abstract

Introduction

Conclusions

References

Tables

Figures

⏪

⏩

◀

▶

Back

Close

Full Screen / Esc

Printer-friendly Version

Interactive Discussion



the ENSEMBLES RCMs, we refer to Klein Tank et al. (2009) and references therein. The estimates of the climatological annual cycle using a 31d MA show high frequency fluctuations in the CTL and SCE periods, which are amplified in the annual cycle of ΔP due to the division of SCE by CTL values. A spurious amplification can be seen at the station LUG in mid October, when a decrease of P in the CTL period and a rapid increase in the SCE period occur, leading to a spike in ΔP . The HO 3 estimate is not influenced by such high frequency fluctuations and results in a smooth annual cycle.

Figure 6 shows further examples of strong fluctuations in the 31d MA around the spectrally smoothed annual cycle ΔP at different station sites and for various model chains. The fluctuations of the 31d MA estimates relative to the spectrally smoothed annual cycles are in the same order of magnitude as the climate change signal.

In the spectral smoothing methodology, overshootings can occur in situations when sudden changes in a time series occur within a time scale that cannot be resolved by the spectral model. In our study, serious overshooting problems occurred in the case of pronounced summer dryings mainly in Southern Switzerland for model chains driven by the GCM HadCM3Q16. In principle, we could resolve the overshooting problem by a root transformation of the P data. However, such a transformation causes the harmonic smoothing to be non-conservative. We therefore chose not to use a root transformation and exclude the model chains driven by HadCM3Q16 in the current analysis.

5.3 Climate change signal at Swiss station sites

5.3.1 Annual cycle of the climate change signal

For brevity, we show results of the climate change signal's annual cycle only at the two exemplary stations BER and LUG (see Fig. 1). Figures 7 and 8 show each RCM's annual cycle of ΔT and ΔP , respectively for both SCE periods relative to the CTL period 1980–2009. To compare the changes to the natural variability range, we resampled each station's observed precipitation record of the CTL period. We constructed

Spectral representation of the annual cycle in the climate change signal

T. Bosshard et al.

Title Page

Abstract

Introduction

Conclusions

References

Tables

Figures



Back

Close

Full Screen / Esc

Printer-friendly Version

Interactive Discussion



100 realisations with a length of 30 years by resampling with replacement the years of the observed record. From the 100 realisations, we randomly chose 500 pairs and estimated the climate change signal between the pairs. The range of ± 1 standard deviation (σ) of the 500 resampled realisations is shown as a grey band in Figs. 7 and 8.

5 In the case of ΔT , the ensemble mean shows peaks in winter and summer in both SCE periods. The model spread is largest in summer, which is mainly due to a strong summer warming of HadCM3Q0-driven experiments. Generally, the ΔT signal for both SCE periods is distinctively above the estimated natural variability range.

10 For ΔP , the GCM dominates the climate change signal as can be seen by model chains that use the RCM RCA. The natural variability range of ΔP is much larger relative to the projected ΔP values than in the case of ΔT . Furthermore, the range of natural variability strongly differs from station to station. Only the projected decrease of P in the summer for the later scenario period is larger than the natural variability for the majority of the RCMs.

15 5.3.2 Spatial patterns of seasonal mean changes

Figures 9 and 10 show the mean seasonal pattern of ΔT and ΔP for both scenario periods. Only the results for the season DJF and JJA are shown since the analysis of the annual cycles showed these seasons to have stronger climate change signals than the transition seasons.

20 For ΔT , the spatial pattern is homogenous across Switzerland with the exception of the Alpine ridge region in JJA that generally shows higher ΔT than other regions in Switzerland. The strongest warming is projected for JJA. The median of all station's ensemble mean ΔT for JJA is 1.4 K for 2021–2050 and 3.7 K for 2070–2099. At most stations, the ensemble mean ΔT is larger than 2 times the standard deviation of the
25 natural variability for both scenario periods.

The strongest seasonal ΔP signal is projected for JJA in the SCE period 2070–2099 with ensemble mean ΔP values around 0.8 in large parts of Switzerland. Southern Switzerland is projected to have the strongest decrease of summer precipitation, with

Spectral representation of the annual cycle in the climate change signal

T. Bosshard et al.

Title Page

Abstract

Introduction

Conclusions

References

Tables

Figures



Back

Close

Full Screen / Esc

Printer-friendly Version

Interactive Discussion



ΔP values around 0.7. For DJF, an increase of P can be expected but the strength of the signal is smaller than for JJA. In the period 2021–2050, the ΔP values generally do not exceed the range of estimated natural variability.

The ensemble mean's projected seasonal changes for the SCE period 2070–2099 are consistent with the results from the PRUDENCE project (Christensen et al., 2007). In the PRUDENCE project, the ensemble mean ΔT in the Alpine region for the SCE period 2070–2100 relative to the CTL period 1961–1990 was +2 K for winter and +4 K for summer. The estimated ensemble mean ΔP was +10% and –30% for winter and summer, respectively (Christensen and Christensen, 2007).

6 Summary and conclusions

The delta change method commonly used in climate impact modelling studies requires a representation of the climate change signal's annual cycle. This implies the estimation of the annual cycle of T and P both in the CTL and the SCE period. Using a stochastic rainfall generator, we showed that climate change signals of mean precipitation derived by moving averages are strongly affected by sampling artefacts. Spatial aggregation to a region corresponding to the area of a few RCM grid cells does not reduce the effect of sampling variability on the climate change signal substantially.

Climate change signals estimated using MAs or fixed averaging intervals such as, for e.g., monthly values should thus be regarded with caution, since associated artificial peaks in the annual cycle can lead to undesirable effects when used in combination with non-linear impact models.

We used a spectral smoothing to ameliorate the effects of natural variability on artificial fluctuations in the annual cycle. Compared to 31d MA estimates, the spectral smoothing successfully filters intraannual fluctuations. In a few cases when a strong amplitude of the annual precipitation cycle is paired with a large relative precipitation change, the spectral smoothing produces overshootings.

Spectral representation of the annual cycle in the climate change signal

T. Bosshard et al.

Title Page

Abstract

Introduction

Conclusions

References

Tables

Figures



Back

Close

Full Screen / Esc

Printer-friendly Version

Interactive Discussion



Spectral representation of the annual cycle in the climate change signal

T. Bosshard et al.

Title Page

Abstract

Introduction

Conclusions

References

Tables

Figures

⏪

⏩

◀

▶

Back

Close

Full Screen / Esc

Printer-friendly Version

Interactive Discussion

The derived climate change signal for the ENSEMBLES GCM-RCM chains is particularly clear for the later SCE period 2070–2099. The peak in the ensembles mean's ΔT is around 4 K. In the case of P , a pronounced decrease of summer precipitation is projected for the whole of Switzerland. In the other seasons, precipitation is projected to increase.

We focussed on changes in the annual cycle of mean T and P as used in the delta change method. This is a statistical model on the lowest complexity level in the whole variety of statistical post-processing methods. It is a general rule that the more complex models become, for e.g., the more parameters they have, the more prone they are to overfitting. Therefore, it is likely that other post-processing methods such as quantile-based de-biasing methods are also affected by artificial fluctuations in the annual cycle of projected changes. Hence, the representation of the annual cycle in any statistical post-processing or downscaling method should be addressed with care.

Acknowledgements. This study was partly funded by swisselectric research, the Federal Office for the Environment (FOEN) and NCCR climate, a research instrument of the Swiss National Science Foundation. The ENSEMBLES data used in this work was funded by the EU FP6 Integrated Project ENSEMBLES (Contract number 505539) whose support is gratefully acknowledged. The observational station data were provided by MeteoSwiss, the Swiss Federal Office of Meteorology and Climatology. We would also like to thank Lukas Rosinus from the statistical seminar of the ETH Zurich for his assistance.

References

- Allen, M. R. and Ingram, W. J.: Constraints on future changes in climate and the hydrologic cycle, *Nature*, 419, 224–232, 2002. 1162
- Buytaert, W., Vuille, M., Dewulf, A., Urrutia, R., Karmalkar, A., and Célleri, R.: Uncertainties in climate change projections and regional downscaling in the tropical Andes: implications for water resources management, *Hydrol. Earth Syst. Sci.*, 14, 1247–1258, doi:10.5194/hess-14-1247-2010, 2010. 1162

Spectral representation of the annual cycle in the climate change signal

T. Bosshard et al.

[Title Page](#)

[Abstract](#)

[Introduction](#)

[Conclusions](#)

[References](#)

[Tables](#)

[Figures](#)

[⏪](#)

[⏩](#)

[◀](#)

[▶](#)

[Back](#)

[Close](#)

[Full Screen / Esc](#)

[Printer-friendly Version](#)

[Interactive Discussion](#)



- Cameron, D., Beven, K., and Naden, P.: Flood frequency estimation by continuous simulation under climate change (with uncertainty), *Hydrol. Earth Syst. Sci.*, 4, 393–405, doi:10.5194/hess-4-393-2000, 2000. 1163
- Christensen, J. H. and Christensen, O. B.: A summary of the PRUDENCE model projections of changes in European climate by the end of this century, *Climatic Change*, 81, 7–30, 2007. 1176
- Christensen, J. H., Carter, T. R., Rummukainen, M., and Amanatidis, G.: Evaluating the performance and utility of regional climate models: the PRUDENCE project, *Climatic Change*, 81, 1–6, 2007. 1176
- Fowler, H. J., Blenkinsop, S., and Tebaldi, C.: Linking climate change modelling to impacts studies: recent advances in downscaling techniques for hydrological modelling, *Int. J. Climatol.*, 27, 1547–1578, 2007. 1162
- Gleick, P. H.: Methods for evaluating the regional hydrologic impacts of global climatic changes, *J. Hydrol.*, 88, 97–116, 1986. 1164
- Graham, L. P., Hagemann, S., Jaun, S., and Beniston, M.: On interpreting hydrological change from regional climate models, *Climatic Change*, 81, 97–122, 2007. 1163, 1165
- Hay, L. E., Wilby, R. L., and Leavesley, G. H.: A comparison of delta change and downscaled GCM scenarios for three mountainous basins in the United States, *J. Am. Water Resour. As.*, 36, 387–397, 2000. 1162, 1164
- Jasper, K., Calanca, P., Gaylistras, D., and Fuhrer, J.: Differential impacts of climate change on the hydrology of two alpine river basins, *Clim. Res.*, 26, 113–129, 2004. 1163
- Kay, A. L., Jones, R. G., and Reynard, N. S.: RCM rainfall for UK flood frequency estimation, II. Climate change results, *J. Hydrol.*, 318, 163–172, doi:10.1016/j.jhydrol.2005.06.013, 2006. 1162
- Kilsby, C. G., Jones, P. D., Burton, A., Ford, A. C., Fowler, H. J., Harpham, C., James, P., Smith, A., and Wilby, R. L.: A daily weather generator for use in climate change studies, *Environ. Modell. Softw.*, 22, 1705–1719, doi:10.1016/j.envsoft.2007.02.005, 2007. 1164
- Klein Tank, A. M. G., Manzini, E., Braconnot, P., Doblas-Reyes, F., Buishand, T. A., and Morse, A.: Evaluation of the ENSEMBLES Prediction System, chap. 8, Met Office Hadley Centre, FitzRoy Road, Exeter, EX1 3PB, UK, 2009. 1174
- Kleinn, J., Frei, C., Gurtz, J., Lüthi, D., Vidale, P. L., and Schär, C.: Hydrologic simulations in the Rhine basin driven by a regional climate model, *J. Geophys. Res.*, 110, D04102, doi:10.1029/2004JD005143, 2005. 1163

Spectral representation of the annual cycle in the climate change signal

T. Bosshard et al.

Title Page

Abstract

Introduction

Conclusions

References

Tables

Figures

⏪

⏩

◀

▶

Back

Close

Full Screen / Esc

Printer-friendly Version

Interactive Discussion



- Kundzewicz, Z. W., Mata, L. J., Arnell, N., Döll, P., Kabat, P., Jiménez, B., Miller, K., Oki, T., Sen, Z., and Shiklomanov, I.: Freshwater resources and their management, in: Climate Change 2007: Impacts, Adaptation and Vulnerability. Contribution of Working Group II to the Fourth Assessment Report of the Intergovernmental Panel on Climate Change, edited by: Parry, M. L., Canziani, O. F., Palutikof, J. P., van der Linden, P. J., and Hanson, C. E., Cambridge University Press, Cambridge, UK, 173–210, 2007. 1162
- Lenderink, G., Buishand, A., and van Deursen, W.: Estimates of future discharges of the river Rhine using two scenario methodologies: direct versus delta approach, *Hydrol. Earth Syst. Sci.*, 11, 1145–1159, doi:10.5194/hess-11-1145-2007, 2007. 1164
- Leung, L. R., Qian, Y., Bian, X., Washington, W. M., Han, J., and Roads, J. O.: Mid-century ensemble regional climate change scenarios for the western United States, *Climatic Change*, 62, 75–113, 2004. 1162
- Middelkoop, H., Daamen, K., Gellens, D., Grabs, W., Kwadijk, J. C. J., Lang, H., Parmet, B. W. A. H., Schädler, B., Schulla, J., and Wilke, K.: Impact of climate change on hydrological regimes and water resources management in the Rhine basin, *Climatic Change*, 49, 105–128, 2001. 1163
- Narapusetty, B., DelSole, T., and Tippet, M. K.: Optimal Estimation of the Climatological Mean, *J. Climate*, 22, 4845–4859, doi:10.1175/2009JCLI2944.1, 2009. 1168, 1172
- Prudhomme, C. and Davies, H.: Assessing uncertainties in climate change impact analyses on the river flow regimes in the UK, Part 1: baseline climate, *Climatic Change*, 93, 177–195, doi:10.1007/s10584-008-9464-3, 2009. 1163
- Prudhomme, C., Reynard, N., and Crooks, S.: Downscaling of global climate models for flood frequency analysis: where are we now?, *Hydrol. Process.*, 16, 1137–1150, doi:10.1002/hyp.1054, 2002. 1164
- Schmidli, J., Goodess, C. M., Frei, C., Haylock, M. R., Hundscha, Y., Ribalaygua, J., and Schmith, T.: Statistical and dynamical downscaling of precipitation: an evaluation and comparison of scenarios for the European Alps, *J. Geophys. Res.*, 112, D04105, doi:10.1029/2005JD007026, 2007. 1163
- Terink, W., Hurkmans, R. T. W. L., Torfs, P. J. J. F., and Uijlenhoet, R.: Evaluation of a bias correction method applied to downscaled precipitation and temperature reanalysis data for the Rhine basin, *Hydrol. Earth Syst. Sci.*, 14, 687–703, doi:10.5194/hess-14-687-2010, 2010. 1163

Spectral representation of the annual cycle in the climate change signal

T. Bosshard et al.

Title Page

Abstract

Introduction

Conclusions

References

Tables

Figures

⏪

⏩

◀

▶

Back

Close

Full Screen / Esc

Printer-friendly Version

Interactive Discussion



van der Linden, P. and Mitchell, J.: ENSEMBLES: Climate Change and its Impacts: Summary of research and results from the ENSEMBLES Project, Met Office Hadley Centre, FitzRoy Road, Exeter, EX1 3PB, UK, 2009. 1164

von Storch, H. and Zwiers, F. W.: Statistical Analysis in Climate Research, Cambridge University Press, UK, 1999. 1168

Wentz, F. J., Ricciardulli, L., Hilburn, K., and Mears, C.: How much more rain will global warming bring, *Science*, 317, 233, doi:10.1126/science.1140746, 2007. 1162

Widmann, M. L., Bretherton, C. S., and Salathé Jr., E. P.: Statistical precipitation downscaling over the northwestern United States using numerically simulated precipitation as a predictor, *J. Climate*, 16, 799–816, 2003. 1163

Wild, M., Grieser, J., and Schär, C.: Combined surface solar brightening and increasing greenhouse effect support recent intensification of the global land-based hydrological cycle, *Geophys. Res. Lett.*, 35, L17706, doi:10.1029/2008GL034842, 2008. 1162

Wilks, D. S.: *Statistical Methods in the Atmospheric Sciences*, vol. 91 of International Geophysics Series, 2nd edition, Academic Press, 30 Corporate Drive, Suite 400, Burlington, MA 01803, USA, 2006. 1172

Wilks, D. S. and Wilby, R. L.: The weather generation game: a review of stochastic weather models, *Prog. Phys. Geog.*, 23, 329–357, 1999. 1169

Wood, A. W., Leung, L. R., Sridhar, V., and Lettenmaier, D. P.: Hydrologic implications of dynamical and statistical approaches to downscaling climate model outputs, *Climate Change*, 62, 189–216, 2004. 1162, 1163

Spectral representation of the annual cycle in the climate change signal

T. Bosshard et al.

Table 2. Seasonal parameter settings of the rainfall generator for the four experiments CHN_{STATION}, CHN_{REGION}, CHS_{STATION} and CHS_{REGION}.

Experiment ID	DJF				MAM				JJA				SON			
	ρ_{ww}	ρ_{dw}	α	β												
CHN _{STATION}	0.55	0.20	1.56	4.26	0.54	0.26	1.47	5.52	0.51	0.26	1.32	7.85	0.51	0.22	1.34	6.92
CHN _{REGION}	0.67	0.23	1.55	4.72	0.66	0.32	1.61	4.39	0.65	0.33	1.55	5.50	0.63	0.24	1.45	5.60
CHS _{STATION}	0.51	0.10	1.05	11.99	0.58	0.19	1.10	13.41	0.50	0.21	0.97	18.10	0.60	0.15	0.96	18.57
CHS _{REGION}	0.54	0.12	0.95	11.69	0.62	0.22	0.96	14.17	0.60	0.28	0.95	13.70	0.65	0.17	0.87	21.40

Title Page

Abstract

Introduction

Conclusions

References

Tables

Figures

⏪

⏩

◀

▶

Back

Close

Full Screen / Esc

Printer-friendly Version

Interactive Discussion

Spectral representation of the annual cycle in the climate change signal

T. Bosshard et al.

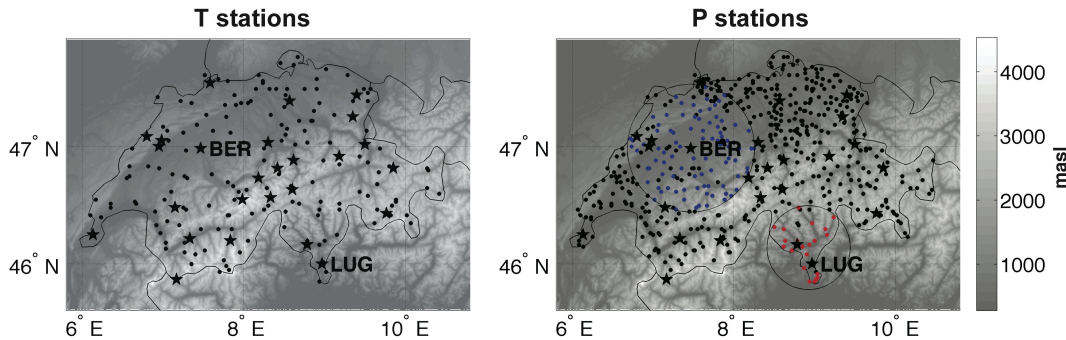


Fig. 1. Map with station locations for T (left) and P (right). Stars indicate stations belonging to the long-term Swiss climate monitoring network. Blue and red dots show the selected stations for the $\text{CHN}_{\text{REGION}}$ (93 stations) and $\text{CHS}_{\text{REGION}}$ (23 stations) experiments, respectively (see Sect. 4).

Title Page

Abstract

Introduction

Conclusions

References

Tables

Figures

⏪

⏩

◀

▶

Back

Close

Full Screen / Esc

Printer-friendly Version

Interactive Discussion

Spectral representation of the annual cycle in the climate change signal

T. Bosshard et al.

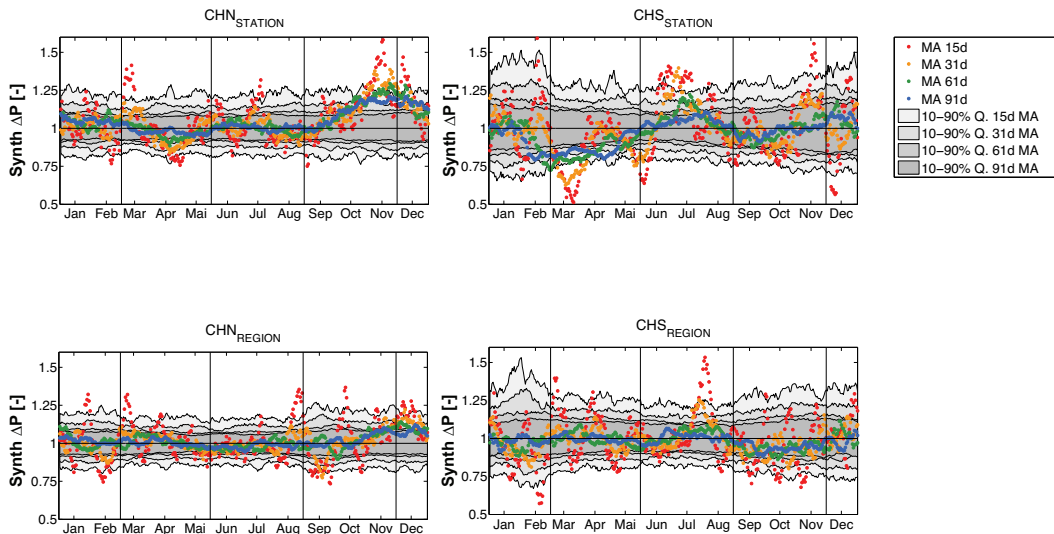


Fig. 2. Annual cycles of the multiplicative precipitation change signals ($\text{Synth } \Delta P$) for the four experiments $\text{CHN}_{\text{STATION}}$, $\text{CHS}_{\text{STATION}}$, $\text{CHN}_{\text{REGION}}$, $\text{CHS}_{\text{REGION}}$ estimated from time series pairs generated by a stationary first order Markov chain rainfall generator. The correct asymptotic solution is one representing no change. The dots indicate a specific realisation whereas the grey bands show the 10th–90th quantile range of 500 realisations. The precipitation change signals were estimated by moving averages (MA) based on averaging window widths of 15, 31, 61 and 91 days over 30 years of daily data.

Title Page

Abstract

Introduction

Conclusions

References

Tables

Figures

⏪

⏩

◀

▶

Back

Close

Full Screen / Esc

Printer-friendly Version

Interactive Discussion

Spectral representation of the annual cycle in the climate change signal

T. Bosshard et al.

Title Page	
Abstract	Introduction
Conclusions	References
Tables	Figures
⏪	⏩
◀	▶
Back	Close
Full Screen / Esc	
Printer-friendly Version	
Interactive Discussion	

Discussion Paper | Discussion Paper | Discussion Paper | Discussion Paper | Discussion Paper

MSE_{CV} for T series at climate stations

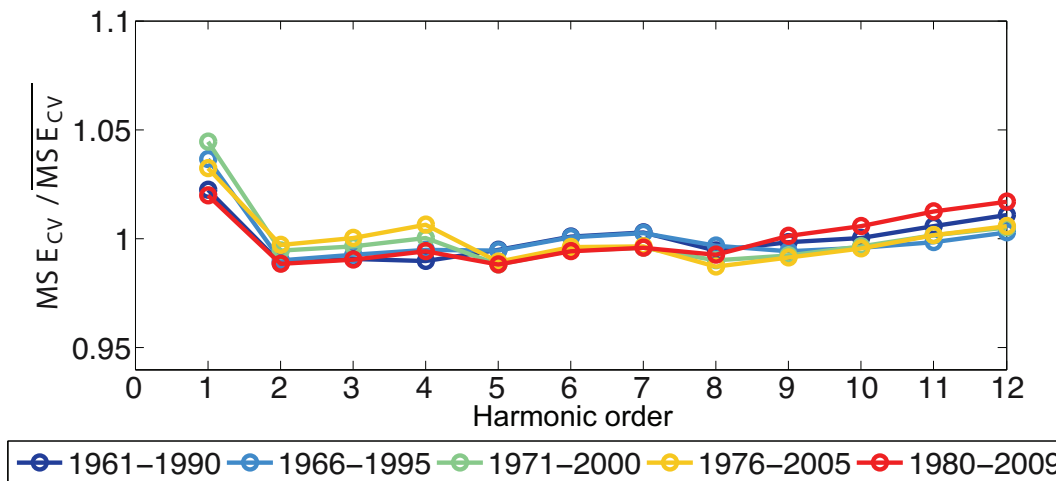


Fig. 3. Mean over all station's MSE_{CV} of harmonic models with increasing harmonic order (HO 1 to HO 12) for observed daily *T* series at Swiss climate monitoring stations (see Fig. 1). Results of five 30 year periods are shown in different colours. The MSE_{CV} have been normalised by the mean MSE_{CV} for display reasons. The MSE_{CV} of HO 0 is much larger compared to higher order harmonic models and is therefore not shown.



Spectral representation of the annual cycle in the climate change signal

T. Bosshard et al.

Title Page	
Abstract	Introduction
Conclusions	References
Tables	Figures
◀	▶
◀	▶
Back	Close
Full Screen / Esc	
Printer-friendly Version	
Interactive Discussion	

Discussion Paper | Discussion Paper | Discussion Paper | Discussion Paper | Discussion Paper

MSE_{CV} for P series at climate stations

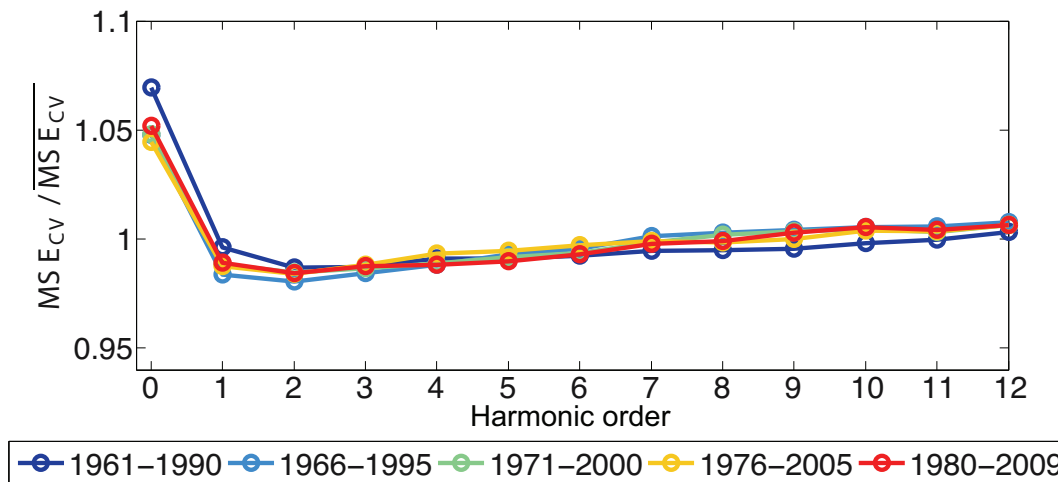


Fig. 4. As Fig. 3 but for observed daily P series at Swiss climate monitoring stations.



Spectral
representation of the
annual cycle in the
climate change signal

T. Bosshard et al.

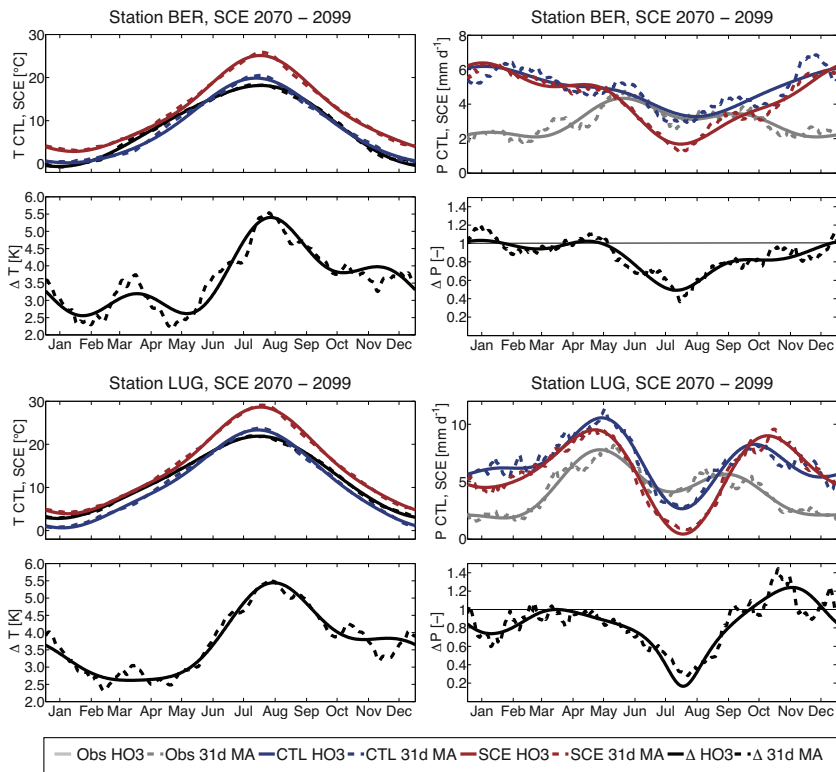


Fig. 5. Comparison between annual cycles estimated by a 31d MA (dashed lines) and a third order harmonic smoothing (HO3; solid lines). Annual cycles of T and P are displayed in the left and right panels, respectively. Results of the model chain ETHZ-HadCM3Q0-CLM at the two exemplary stations BER (top) and LUG (bottom) are shown. In each of the four blocks, the top panels contain the annual cycles in the CTL period 1980–2009 and SCE period 2070–2099. The annual cycles of the observed records in the CTL period are added in grey. In the bottom panels, the delta change signals are shown.

Title Page

Abstract

Introduction

Conclusions

References

Tables

Figures

◀

▶

◀

▶

Back

Close

Full Screen / Esc

Printer-friendly Version

Interactive Discussion

Spectral representation of the annual cycle in the climate change signal

T. Bosshard et al.

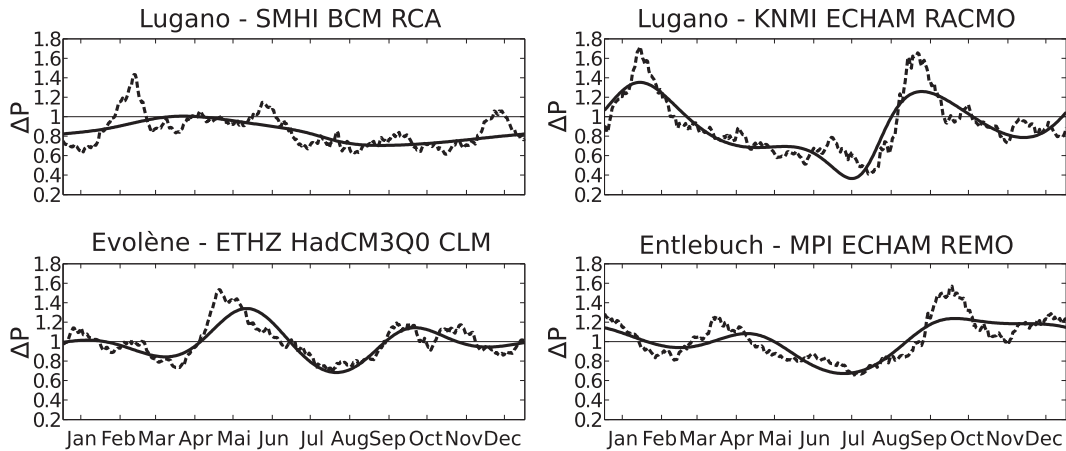


Fig. 6. Examples of ΔP as estimated by 31d MA (dashed lines) and the spectral smoothing (solid lines) of various model chains at different station sites as indicated in each panel's title. Examples are shown for the SCE period 2070–2099.

Title Page

Abstract

Introduction

Conclusions

References

Tables

Figures

◀

▶

◀

▶

Back

Close

Full Screen / Esc

Printer-friendly Version

Interactive Discussion

Spectral representation of the annual cycle in the climate change signal

T. Bosshard et al.

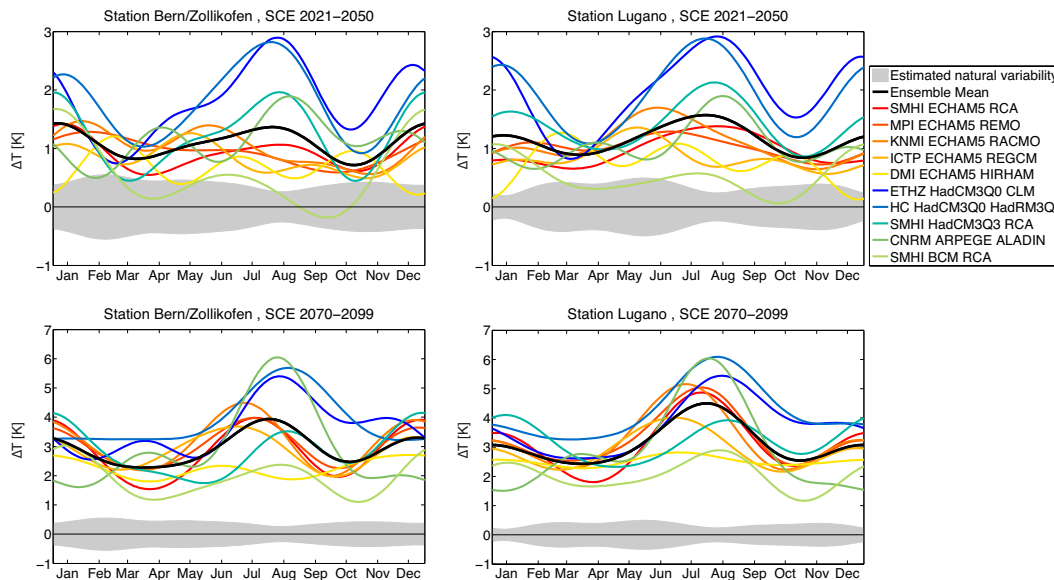


Fig. 7. Annual cycle of ΔT for the scenario period 2021–2050 (top) and 2070–2099 (bottom) at the two exemplary stations BER (left) and LUG (right). Each of the 10 GCM-RCMs is shown with an individual colour. The ensemble mean is indicated by a black line. The grey band shows the range of the estimated natural variability as $\pm\sigma$ of the resampled ΔT s at the station site. Note the different scales in upper and lower panels.

Title Page

Abstract Introduction

Conclusions References

Tables Figures

◀ ▶

◀ ▶

Back Close

Full Screen / Esc

Printer-friendly Version

Interactive Discussion

Spectral representation of the annual cycle in the climate change signal

T. Bosshard et al.

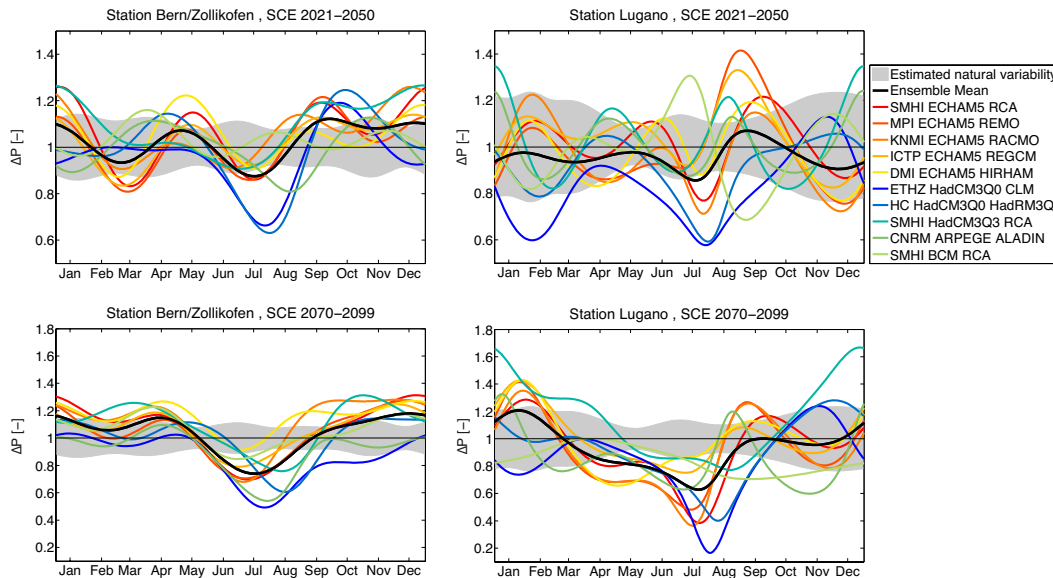


Fig. 8. Same as Fig. 7 but for ΔP .

Title Page

Abstract

Introduction

Conclusions

References

Tables

Figures

◀

▶

◀

▶

Back

Close

Full Screen / Esc

Printer-friendly Version

Interactive Discussion

Spectral representation of the annual cycle in the climate change signal

T. Bosshard et al.

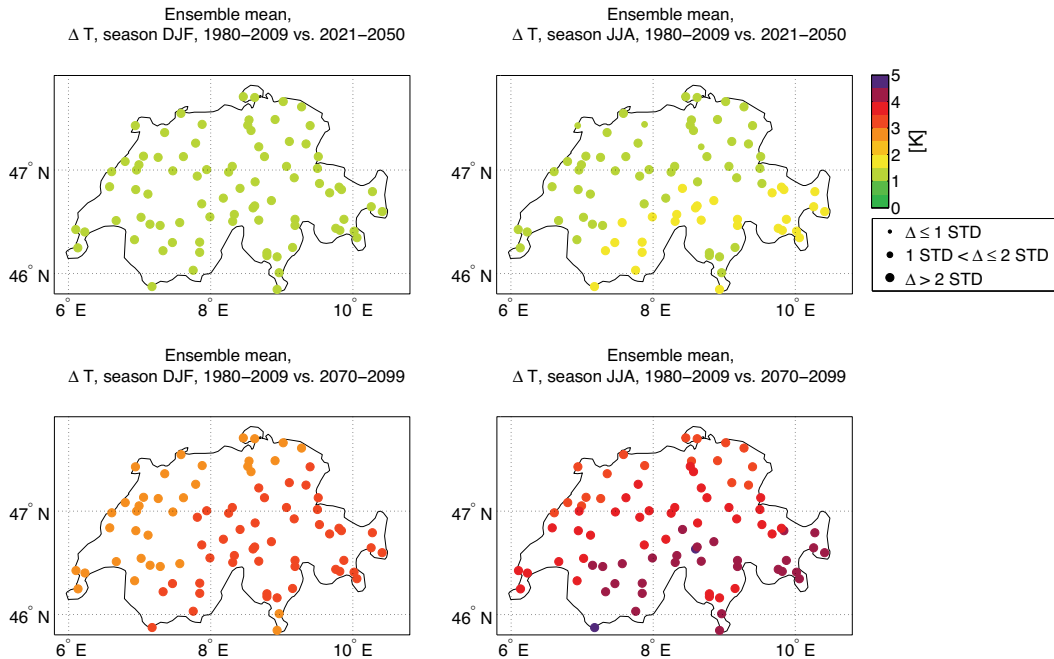


Fig. 9. Seasonal ensemble mean ΔT at all station sites for both scenario periods 2021–2050 (top) and 2070–2099 (bottom) and the seasons DJF (left) and JJA (right). The colour scale indicates the ensemble mean value of ΔT . The size of the dot indicates the magnitude of ΔT relative to the standard deviation (STD) of the estimated natural variability at the respective station. At stations having more than 10% missing values, no natural variability was estimated. These stations are not shown.

[Title Page](#)

[Abstract](#) [Introduction](#)

[Conclusions](#) [References](#)

[Tables](#) [Figures](#)

[◀](#) [▶](#)

[◀](#) [▶](#)

[Back](#) [Close](#)

[Full Screen / Esc](#)

[Printer-friendly Version](#)

[Interactive Discussion](#)



Spectral representation of the annual cycle in the climate change signal

T. Bosshard et al.

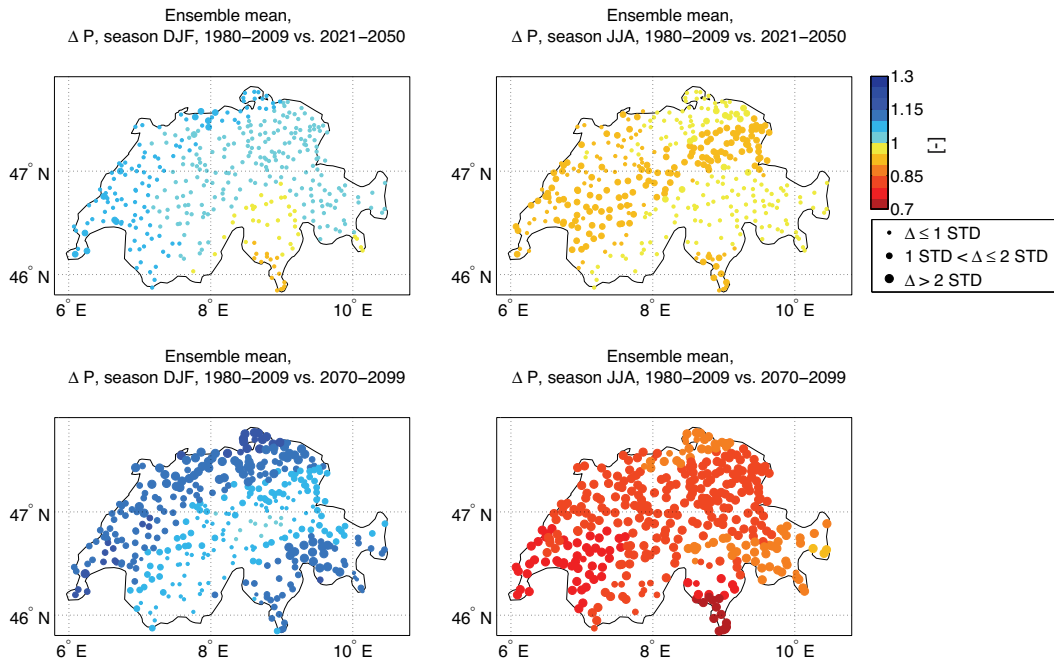


Fig. 10. Same as Fig. 9 but for the seasonal ensemble mean ΔP .

Title Page

Abstract

Introduction

Conclusions

References

Tables

Figures

◀

▶

◀

▶

Back

Close

Full Screen / Esc

Printer-friendly Version

Interactive Discussion